Journal of Quality Measurement and Analysis *JQMA* 2020 16(2), 193-206
e-ISSN: 2600-8602 *http://www.ukm.my/jqma*

PROJECTION OF TEMPERATURE IN RELATION TO CARDIOVASCULAR DISEASE USING BIAS CORRECTION METHOD

(Unjuran Suhu dalam Hubungan dengan Penyakit Kardiovaskular Menggunakan Kaedah Pembetulan Pincang)

AINA IZZATI MOHD ESA, SYAFRINA ABDUL HALIM*, NORZAIDA ABAS, JING XIANG CHUNG & MOHD SYAZWAN FAISAL MOHD

ABSTRACT

Climate and weather have significant influences on human health. Climate change together with natural phenomena and human activities have the tendency to impact the environment and debilitates human well-being in various ways. Extreme temperature, which is often associated with climate change, has some negative implications on human health, potentially resulting in diseases such as cardiovascular disease. The aim of this study is to analyze the impacts of temperature projection on the mortality rates of cardiovascular disease based on daily average temperature projection using bias correction method. Downscaling approach can be used to downscale the global climate model outputs that are available at coarse resolution. However, to study the impact of climate change need meteorological data or information at finer resolution. In this study, statistical downscaling is used to downscale the GCM's temperature to local scale's temperature. The observed daily mean temperature data in 5 years (1970- 1974), the historical GCM data (1976-1980) and the projection data (2076-2080) under RCP4.5 and RCP8.5 were used. However, the global climate model outputs produce biases when applied due to its coarse estimate, hence lead to erroneous results. Thus, bias correction method was used to correct the biases in global climate model outputs to project the future of extreme temperature, and eventually calculate the mortality rate of the cardiovascular diseases. The mortality rate of the cardiovascular disease is calculated by using attributable daily deaths formula. Results revealed that quantile mapping technique is able to capture the variability in global climate model as well as quantifying the biases. The projected trend of heat-related deaths under RCP4.5 is lower than the deaths under RCP8.5.

Keywords: global climate model; bias correction method; quantile mapping; temperature; mortality

ABSTRAK

Iklim dan cuaca mempunyai pengaruh yang penting terhadap kesihatan manusia. Perubahan iklim bersama dengan fenomenon semula jadi dan aktiviti manusia mempunyai kecenderungan memberi impak kepada persekitaran dan mengganggu kesihatan manusia dalam pelbagai cara. Suhu yang melampau yang selalu dikaitkan dengan impak perubahan iklim, membawa implikasi negatif terhadap kesihatan manusia termasuk berpotensi menyebabkan penyakit seperti penyakit kardiovaskular. Tujuan kajian ini adalah untuk menganalisis impak unjuran suhu ke atas kadar kematian penyakit kardiovaskular berdasarkan unjuran suhu purata harian menggunakan kaedah pembetulan pincang. Pendekatan penurunan skala boleh digunakan untuk penurunan output dari model iklim global yang boleh didapati pada resolusi kasar. Walau bagaimanapun, untuk mengkaji impak perubahan iklim memerlukan maklumat meteorologi pada skala yang lebih kecil. Dalam kajian ini, pendekatan penurunan secara statistik digunakan untuk menurunkan suhu model iklim global kepada suhu pada skala tempatan. Nilai purata harian yang dicerap untuk 5 tahun (1970-1974), data sejarah purata suhu harian model iklim global (1976-1980) dan data peramalan purata suhu harian untuk RCP4.5 dan RCP8.5 telah diguna. Bagaimanapun output daripada model iklim global adalah pincang kerana ia bersifat anggaran kasar dan boleh

The study reported in this paper was presented at the 27th National Symposium on Mathematical Sciences (SKSM27) at Hotel Tenera, Bangi, Selangor on 26 - 27 November 2019, organised by Department of Mathematics, Faculty of Science, Universiti Putra Malaysia.

mengakibatkan keputusan yang salah. Oleh itu, kaedah pembetulan pincang telah digunakan untuk memperbetulkan output daripada model iklim global untuk unjuran suhu melampau masa akan datang, dan seterusnya diguna dalam pengiraan kadar kematian disebabkan oleh penyakit kardiovaskular. Kadar kematian penyakit kardiovaskular dikira dengan menggunakan rumus kematian harian diatribut. Keputusan menunjukkan bahawa teknik pemetaan kuantil berupaya menangani kebolehubahan dalam model iklim global serta mengira kepincangan. Trend unjuran kematian berkaitan dengan suhu untuk RCP4.5 didapati lebih rendah daripada yang RCP8.5.

Kata kunci: model iklim global; kaedah pembetulan pincang; pemetaan kuantil; suhu; kematian

1. Introduction

Climate change refers to the considerable change of weather parameters, measured over multiple decades. Climate change varies from decades to decades, normally due to natural phenomena or human activities (Crimmins *et al.* 2016). The impacts of climate change include the frequent occurrence of extreme events such as increase in temperature and changes in precipitation. Climate change also poses significant threats to human health. In early twenty-first century, there was rapid development around the world. Such development may considerably affect the ecosystem of the environment and thus, poses threat to the wellbeing in various ways. In the United States, extreme heat events are one of the events that increased discomfort and fatigue, heat cramps, increase visits emergency room, hospitalization and deaths, based on a study conducted by Center for Disease Control and Prevention (CDC) (Luber & McGeehin 2008). From 1999 until 2009, a total of 7,800 deaths due to extreme heat exposure has been recorded (Luber & McGeehin 2008). Extreme heat is a threat to human health in most countries including Malaysia.

Malaysia is located on the Southeastern Asia, comprises of two regions which are West Malaysia and East Malaysia separated from each other by the South China Sea. Being located on the Earth's equator, Malaysia experiences hot and humid throughout. Warming trend between 2.7℃ -4.0℃/100 years are prominent at several weather stations in Peninsular Malaysia and northern Borneo. Meanwhile, in contrast, lower significant warming trends are more prominent at South western Borneo such as Kuching, Bintulu, and Miri stations with temperature between 1.0℃-1.5℃/100 years (Tang 2019).

The same study also found that the country has experienced multiple extreme weather events such as high temperature, high rainfall, dry spell, thunderstorm, and strong winds from 1980 until 2015. Record of daily temperature in Malaysia showed temperature spikes in 1972, 1991, 1997-1998 and 2015-2016, which coincide with the event of strong El Niño especially in 2015-2016 (Tang 2019). In particular, Subang Jaya recorded the highest magnitude of increase in the annual moving average of daily temperature with temperature between 26℃ to 28.7℃ (1961-2018) followed by Kuantan with 25℃ to 28℃ (1961-2018), Malacca with 26℃ to 28.5℃ (1960-2018), Kota Kinabalu with 26℃ to 28.5℃ (1956-2018) and Kuching with 25.5℃ to 28℃ (1956-2018) (Tang 2019). Higher temperature recorded in Subang Jaya might be due to the high rate of development within the area.

A study of impact of climate change on heat-related mortality was conducted in Jiangsu, China over the period 2016 through 2070. The results have shown that the projected ambient temperatures will continue to increase in 2016-2070 under both RCP4.5 and RCP8.5. In general, RCP8.5 yielded higher daily average temperatures under RCP4.5 and this difference becomes larger over time (Chen *et al.* 2017). RCP4.5 is described as an intermediate scenario where temperature is expected to increase by 1.4℃ in the mid-century on average. Meanwhile, RCP8.5 is decribed as a worst-case climate change scenario where the temperature is expected to increase by 2.0℃ in the mid-century on average. The future changes in projected temperature under both RCP4.5 and RCP8.5 may cause stroke, ischemic heart disease (IHD), other cardiovascular-related and respiratory diseases as well as increase in non-accidental deaths in 2016-2040 and 2041-2065 relative to 1981-2005. Specifically, 1713 and 5314 excess heat-related cardiovascular deaths, 452 and 1286 excess heat-related respiratory deaths, 667 and 2217 excess heat-related stroke deaths, 237 and 787 excess heat- related IHD deaths, and 323 and 964 excess heat-related COPD deaths in 2016-2040 and 2041-2065 respectively under RCP4.5 (Chen *et al.* 2017). More excess heat-related cause- specific deaths are projected under RCP8.5.

2. Cardiovascular Disease (CVD)

Cardiovascular disease (CVD) or known as blood circulatory disease is a group of disorders of the heart and blood vessels (Abdullah *et al.* 2017). According to the World Health Organization (WHO), in 2016, the CVD contributed to the highest percentage on mortality (35%) followed by communicable, maternal, perinatal, and nutritional conditions (17% each) (World Health Organization 2018). Meanwhile, other diseases such as cancers and non-communicable recorded the same percentage which is 16%. One of the CVDs namely coronary heart disease (CHD) is a leading killer disease in Malaysia. According to the Department of Statistics Malaysia (DOSM), CHD was the principal causes of death in 2016 with 13.2%, followed by pneumonia with 12.5%, cerebrovascular diseases with 6.9%, transport accidents with 5.4% and malignant neoplasm of trachea, bronchus, and lung with 2.2% (Kei 2017). In 2017, the percentage of deaths caused by CHD was 13.9%, followed by pneumonia with 12.7%, cerebrovascular diseases with 7.1%, transport accidents with 4.6%, and malignant neoplasm of trachea, bronchus, and lung with 2.3%. CHD still remained as the principal cause of death with 15.6%, followed by pneumonia with 11.8%, cerebrovascular diseases with 7.8%, transport accidents with 3.7%, and chronic lower respiratory diseases with 2.6% in 2018.

Table 1: Percentages of mortality due to types of cardiovascular disease in Malaysia in 2016

Types of cardiovascular disease	Percentages of mortality
Acute rheumatic fever	0.02%
Chronic rheumatic heart disease	0.29%
Hypertensive disease	2.79%
Arteries, veins, lymphatic and lymph nodes disease	3.09%
Pulmonary circulation and other forms of heart disease	23.71%
Coronary heart disease	34.33%
Cerebrovascular disease	35.77%

Table 1 shows that cerebrovascular disease has highest percentage with 35.78% followed by coronary heart disease (34.33%), pulmonary circulation and other forms of heart disease (23.71%), arteries, veins, lymphatic and lymph nodes disease (3.08%), hypertensive disease (2.79%), chronic rheumatic heart disease (0.29%) and acute rheumatic fever (0.03%). This can be concluded that, not only coronary heart disease can contribute to elevate the mortality rates in Malaysia, but other CVD can also lead to elevate the mortality rates if not prevented. In the late 21st century, the number of temperature-related CVD deaths is projected to increase under the RCP4.5 and RCP8.5. Extreme heat events could potentially harm human health. Hence, the aim of this study is to analyze the impacts of temperature projection on the mortality rates of CVD based on the temperature projection using bias correction method.

3. Study Area and Data

3.1. *Meteorological Data*

Selangor is the most developed state in Malaysia with highest population and higher standard of living. With rapid development, Selangor has becoming one of the warmest regions in Malaysia with average daily temperature of 33℃. Based on statistics from DOSM, the crude death rate in Selangor increased from 3.9 per 1,000 population to 4.2 per 1,000 population in 3 years (2015-2017) (Department of Statistics Malaysia 2016). In this study, the study area of Selangor is between longitude 100.775°N to 101.975°S and latitude 2.52°E to 3.875°W following the global climate model (GCM) coordinates. Daily temperature data for that particular grid is extracted and used. Figure 1 shows the map of Selangor.

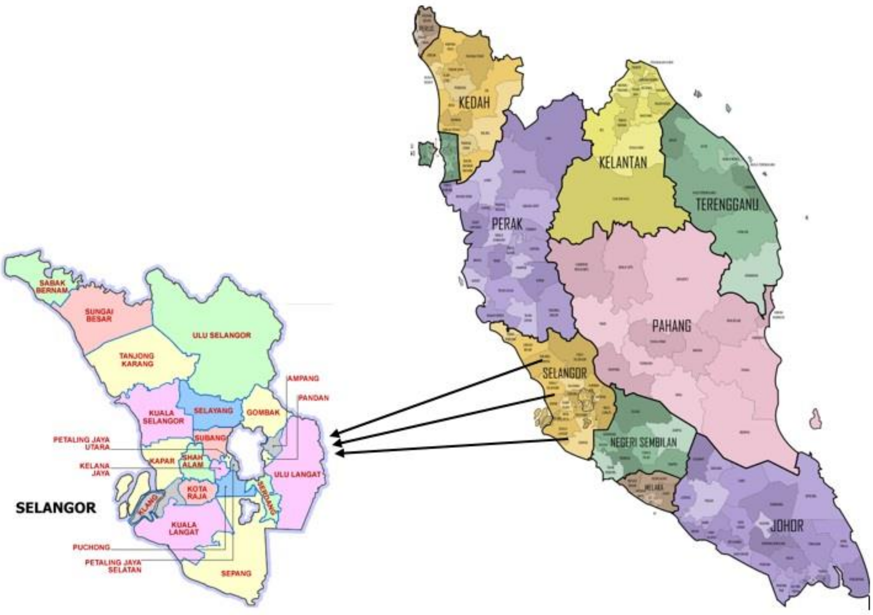

Figure 1: Map of Selangor

Observed daily mean temperature data in 5 years (1970-1974) were obtained from previous study (Wong 2011). Next, output of daily mean temperature for GCM for 5 years were obtained. The historical data were obtained (1976-1980) and the future data were obtained (2076-2080) under two scenarios which are RCP4.5 and RCP8.5. The GCM used in this study is Model for Interdisciplinary Research on Climate (MIROC5) at atmospheric grid which were conducted under the Coupled Model Intercomparison Project Phase 5 (CMIP5). Representative Concentration Pathways (RCPs) is a set of initial values of radiative forcing, carbon dioxide (CO_2) concentration and temperature anomaly and estimated emission up to 2100. RCPs were developed based on assumptions for future economic activity, energy sources, population growth and other socio-economic factors (Wayne 2013). There are four scenarios which are RCP8.5, RCP6.0, RCP4.5 and RCP2.6. In this study, RCP4.5 and RCP8.5 were used because of the high difference in radiative forcing, CO_2 concentration and temperature anomaly. RCP8.5 is characterized as the increasing greenhouse gas emission over time. In contrast, RCP4.5 is characterized as stabilization scenario where the radiative forcing is stabilized shortly after 2100 without overshooting the long-run radiative forcing target level. Radiative forcing measures the influence of a factor that altering the balance of incoming and outgoing energy in the Earth-atmosphere system. Each RCP has a specific emission trajectory and subsequent radiative forcing, as shown in Table 2.

Table 2: Emission trajectory and radiative forcing

RCP	Radiative forcing (Wm^2)	CO_2 concentration ($p.p.m$)	Temperature anomaly (℃)	Pathway
RCP8.5	8.5 in 2100	1370	4.9	Rising
RCP4.5	4.5 post in 2100	650	2.4	Stabilization without overshoot

3.2. *Mortality Data*

This study focused on coronary heart disease (CHD) as CHD is one of the CVD diseases that related to temperature. In this study, mortality data for CHD recorded at the hospital which are National Heart Institute, Kuala Lumpur Hospital, Sultanah Aminah Hospital, University Malaya Medical Centre, Penang Hospital, Sarawak General Hospital, Tuanku Fauziah Hospital, Tunku Ja'afar Hospital, Sultanah Bahiyah Hospital, Raja Perempuan Zainab 2 Hospital, Tengku Ampuan Afzan Hospital, Ipoh Hospital, Queen Elizabeth Hospital, Seberang Jaya Hospital, Sultanah Nur Zahirah Hospital, Tengku Ampuan Rahimah Hospital and Malacca General Hospital from 2011 until 2015 were obtained from the Summary Annual Report NCVD-ACS Registry 2006-2015.

4. Method

GCMs are developed and used as instruments in assessing the large-scale climate characteristics. Unfortunately, coarse horizontal resolution is not suited to represent regional-scale climate characteristics. Thus, there is a need to apply downscaling technique to derive the local scale information from GCMs. Downscaling is utilized to portray the method of relating data or information at relatively coarse spatial and transient scales to the desired products at finer spatial and transient scales (Abatzoglou & Brown 2012). There are two types of downscaling techniques which are statistical and dynamical. Statistical downscaling is the relationship between large-scale parameters that are well resolved by a global model and observations at smaller spatial scales. Meanwhile, dynamical downscaling is a powerful technique due to its ability to explicitly simulate the spatial and transient change ability of changes in meteorological variables and to simulate local changes in temperature or precipitation that are possibly diverse from the climate signals from the global model (Abatzoglou & Brown 2012). However, there exist potential biases in GCMs outputs due to the lack of ensemble. Dynamical downscaling is also computationally intensive. In contrast, statistical downscaling is shown to be more computationally proficient, in which it can straightforwardly consolidate observations used in operational decision-making or modelling (Teutschbein & Seibert 2012). Hence, in this study, statistical downscaling is used to downscale the output from GCM.

4.1. *Bias Correction Method (BCM)*

GCMs output contains biases. These biases can be corrected using the BCM. BCM uses a transformation function or transfer function to identify and correct the possible biases between observed data and simulated climate data (Husak *et al.* 2007). A study by Ajaaj *et al.* (2016), compared several techniques of BCM namely mean bias-remove, multiplicative shift, standardized-reconstruction, linear regression, and quantile mapping. Based on the results, quantile mapping technique and mean bias-remove technique were found to perform better than the other techniques. However, quantile mapping technique was found to give better results during wet and rainy season while mean bias-remove technique gave better result during rainy season only (Husak *et al.* 2007). The quantile mapping technique has proved to efficiently remove biases for the first two statistical moments. This technique was also able to capture the evolution of mean and variability of GCMs (Husak *et al.* 2007). In this technique, the transfer function is fitted with statistical continuous probability distribution function (PDF). This study used Gamma distribution to reduce biases of mean daily temperature. Gamma distribution is positively skewed thus, it could mimic the actual temperature distribution. The PDF of Gamma distribution is

$$f(x) = \frac{\beta^{\alpha} x^{\alpha-1} e^{-\beta x}}{\gamma(\alpha)} \tag{1}$$

where, x is the daily mean temperature, α is the shape parameter, β is the scale parameter and $\gamma(\alpha)$ is the gamma function. The parameters α and β are unknown parameters. The formula of gamma function is

$$\gamma(\alpha) = \int_0^{\infty} x^{\alpha-1} e^{-x}\, dx \tag{2}$$

The cumulative distribution function (CDF) of Gamma distribution needs to be identified. Hence, the CDF of Gamma distribution is

$$F(x) = \frac{\beta^{\alpha}}{\gamma(\alpha)} \int_0^{\infty} t^{\alpha-1} e^{-t}\, dt \tag{3}$$

The steps to find the CDF of Gamma distribution for observed data are as follows:
Step 1: The observed data (1976-1980) according to day, month and year were sorted.
Step 2: The missing values were replaced by mean values.

$$\bar{x} = \frac{\sum_{i=1}^{n} x_i}{n} \tag{4}$$

Step 3: Two parameters for a Gamma distribution,   and   were estimated using Maximum Likelihood Estimation (MLE). The likelihood function is

$$L = \prod_{i=1}^{n} \frac{\beta^{\alpha} x_i^{\alpha-1} e^{-\beta x_i}}{\gamma(\alpha)} \tag{5}$$

$$L = \left(\prod_{i=1}^{n} x_i\right)^{-1} \left(\prod_{i=1}^{n} x_i\right)^{\alpha} e^{-\beta \sum x_i} \beta^{n\alpha} \gamma^{-1}(\alpha) \tag{6}$$

Hence, the log likelihood function is

$$\frac{\delta \ln L}{\delta \alpha} = \sum_{i=1}^{n} \ln x_i + n \ln \beta - n\left(\frac{d}{d\alpha} \ln \gamma(\alpha)\right) = 0 \tag{7}$$

$$\frac{\delta \ln L}{\delta \beta} = -\sum_{i=1}^{n} x_i + \frac{n\alpha}{\beta} = 0 \tag{8}$$

Solving Eq. (7) and (8) results in

$$\ln \alpha - \psi(\alpha) + \overline{\ln x} - \ln \bar{x} = 0 \tag{9}$$

$$\beta = \frac{\alpha}{\bar{x}} \tag{10}$$

where, $\bar{x}$ is the sample mean, $\overline{\ln x} = \sum_{i=1}^{n} \ln x_i / n$ and $\psi(\alpha)$ is digamma function. The formula for digamma function is

$$\psi(\alpha) = \frac{d}{d\alpha} \ln \gamma(\alpha) \tag{11}$$

Eq. (10) can be solved directly but Eq. (9) cannot be solved directly because it is unique. Hence, numerical method (Newton-Raphson method) is applied to solve Eq. (9). The formula of Newton-Raphson method is

$$\alpha^{i+1} = \alpha^{i} - \frac{h(\alpha^{i})}{h'(\alpha^{i})}, i = 1,2,3, \ldots \tag{12}$$

The initial value of α^i can be estimated using Method of Moment (MME). The formula to estimate α^i is

$$\alpha^{i} = \frac{n\bar{x}^2}{\sum_{i=1}^{n} x_i^2 - n\bar{x}^2} \tag{13}$$

Repeat the iteration until the $\left|\alpha^{i+1} - \alpha^{i}\right| < 0.0001$.
Step 4: The CDF of gamma distribution for observed data was identified using Eq. (2).
Step 5: Repeat Step 1 – 4 for historical GCM data.

The similar steps are repeated in order to find the CDF of gamma distribution for historical GCM and future GCM data. The corrected values between observed and historical GCM were calculated using transfer function quantile mapping technique. The formula of transfer function quantile mapping technique is

$$F_{corrected} = \frac{1}{CDF_y}(CDF_z \times z) \tag{14}$$

where, $F_{corrected}$ is the corrected values, y is the simulated GCM data and z is the observed data. Then, the future of mean temperature under RCP4.5 and RCP8.5 are projected by using Eq. (13). The values of observed data (z) were replaced by corrected values ($F_{corrected}$) and the values of historical GCM data (y) were replaced by future data under RCP4.5 (w_1) and RCP8.5 (w_2). Projection future daily mean temperature under RCP4.5 and RCP8.5,

$$F_{projection\ (RCP4.5)} = \frac{1}{CDF_{w_1}}(CDF_{F_{corrected}} \times F_{corrected}) \quad (15)$$

$$F_{projection\ (RCP8.5)} = \frac{1}{CDF_{w_2}}(CDF_{F_{corrected}} \times F_{corrected}) \quad (16)$$

where, w_1 is the future data under RCP4.5 and w_2 is the future data under RCP8.5.

5. Projection of the Impact on Mortality

The estimates of the future (2076-2080) impact of high temperature on mortality rates due to cardiovascular disease were calculated using the attributable daily deaths (ADD) formula which is (Gasparrini *et al.* 2010):

$$ADD = y_0 \times ERC \times POP \quad (17)$$

where, ADD is daily temperature-related to deaths due to cardiovascular disease, y_0 is the baseline mortality due to cardiovascular disease, ERC is the attributable change in mortality due to cardiovascular disease for a specified change in temperature at each temperature and POP is the population value. Distributed lag non-linear model (DLNM) was used to model the relationship between temperature and mortality due to cardiovascular disease. DLNM has an advantage to capture the complex non-linear and lagged dependencies of exposure-response relationships through two-function modeling which are exposure-response and lag-response relationship, respectively. Then, the exposure-response and lag-response relationship are combined in cross-basis function. The exposure-response relationship uses quadratic B-spline while lag response relationship uses natural cubic B-spline. However, in this study the DLNM only consider the exposure-response relationship in calculation. The normalized B-spline basis function is (Gasparrini *et al.* 2010):

$$P(u) = \sum_{i=1}^{n} B_{i,m}(u)\, V_i \quad (18)$$

where, V_i is the ith control point and $B_{i,m}$ are the B-splines blending functions or known as B-splines basis function. The order m can be chosen from 2 to $n + 1$. The basis function $B_{i,m}(u)$ is defined by the recursion formula of Cox-de Boor

$$B_{i,m}(u) = \frac{u - t_i}{t_{i+m-1} - t_i} B_{i,m-1}(u) + \frac{t_{i+m} - u}{t_{i+m} - t_{i+1}} B_{i+1,m+1}(u) \quad (19)$$

where, $t_i \le u \le t_{i+m}$ and

$$B_{i,1}(u) = \begin{cases} 1 & if\ t_i \le u \le t_{i+1} \\ 0 & otherwise \end{cases} \quad (20)$$

The t_is in Eq (20) are elements of a knot vector. From Eq (20), the basis function $B_{i,m}(u)$ is non-zero in the interval $[t_i, t_{i+m}]$.

6. Results and Discussions

Table 3 shows the parameter values for α and β of Gamma distribution and their associated 95% confidence interval for observed, historical GCM and future GCM under RCP4.5 and RCP8.5 scenarios. The confidence interval for each parameter does not include 0 thus indicating that the estimated parameters are significant.

Table 3: Parameters value of Gamma distribution

Data	Parameters value	Standard error	95% confidence interval
Observed	17.8931	0.0244	(17.8930, 17.8931)
	0.0706	0.0001	(0.0706, 0.0706)
Historical	17.6145	0.0245	(17.6144, 17.6145)
	0.0709	0.0001	(0.0709, 0.0709)
RCP4.5	17.6145	0.0245	(17.6144, 17.6145)
	0.0693	0.0001	(0.0693, 0.0693)
RCP8.5	17.3935	0.0237	(17.3935, 17.3936)
	0.0682	0.0001	(0.0682, 0.0682)

Figure 2 shows the mean of monthly average temperature for observed, historical GCM and downscaled values between observed and historical GCM (i.e. corrected values). In January and December, the mean of monthly average temperature for corrected values are higher than the mean of monthly average temperature for observed and historical GCM data while in March and April the mean of monthly average temperature for corrected values are lower than the mean of monthly average temperature for observed and historical GCM data. Meanwhile, in February, May, June, July, August, September, October and November, the mean of monthly average temperature for corrected values are closer to the mean of monthly average temperature for observed data.

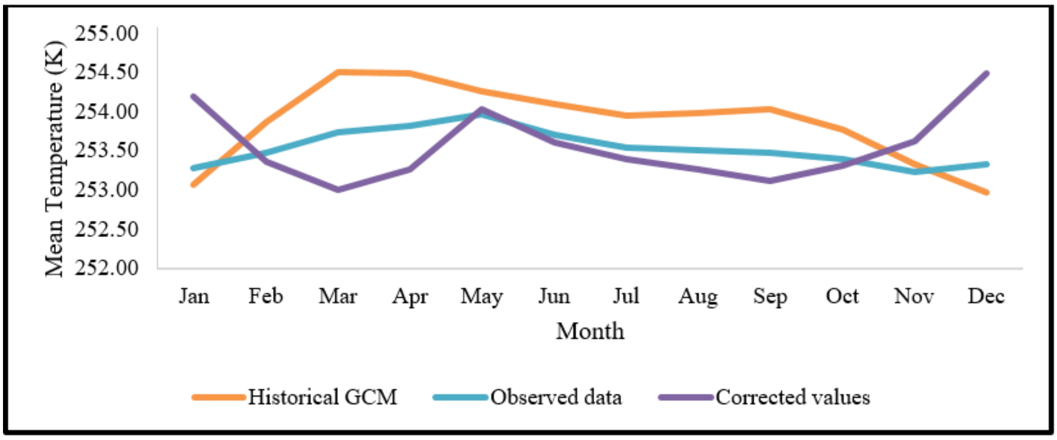

Figure 2: The mean of monthly average temperature for observed, historical GCM and corrected values

Figure 3 shows the mean of monthly average temperature for future GCM and corrected future under RCP4.5. In January and December, the mean of monthly average temperature for corrected future were higher than the mean of monthly average temperature for future GCM while in February and November, the mean of monthly average temperature for corrected future are closer to the mean of monthly average temperature future GCM. In other months, the mean of monthly average temperature for corrected future were lower than the mean of monthly average temperature for future GCM.

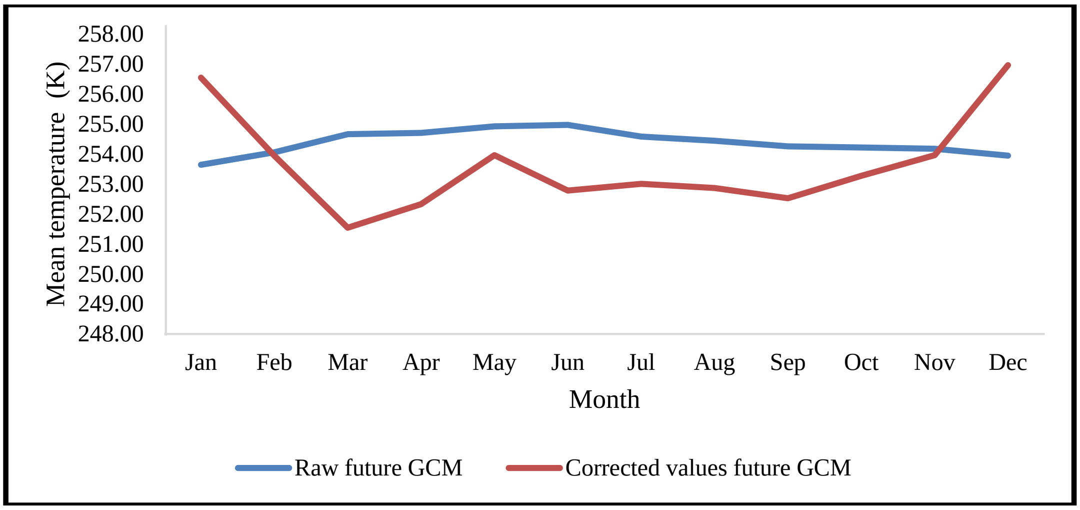

Figure 3: The mean of monthly average temperature for future GCM data and corrected future data under RCP4.5

Figure 4 shows the mean of monthly average temperature for future GCM and corrected future under RCP8.5. The mean of monthly average temperature for corrected future were higher in January and December than the mean of monthly average temperature for future GCM. Only in March, the corrected future is lower than the future GCM. The mean of monthly average temperature for corrected future under in February, April, May, June, July, August, September, October, and November are closer to the mean of monthly average temperature for future GCM.

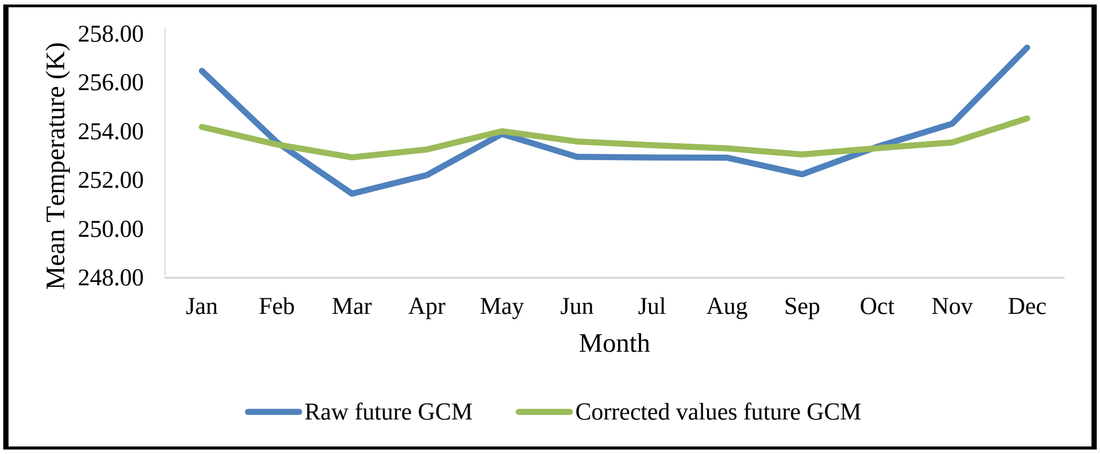

Figure 4: The mean of monthly average temperature for future GCM and corrected future under RCP8.5

Figure 5 shows the line graph of the ADD due to CVD under RCP4.5 and RCP8.5. Based on Figure 5, the projected trend of heat-related deaths under RCP4.5 is found to be increasing from 2076 until 2080. In contrast, the projected trend of heat-related deaths under RCP8.5 is showing decreasing trend from 2076 to 2077 and increasing trend from 2078 to 2080. The figure also shows that, the projected trend of heat-related deaths under RCP4.5 in 2077 and

2078 is higher than the projected trend of heat-related deaths under RCP8.5. Meanwhile, the projected trend of heat-related deaths under RCP4.5 is lower than the projected trend of heat-related deaths under RCP8.5.

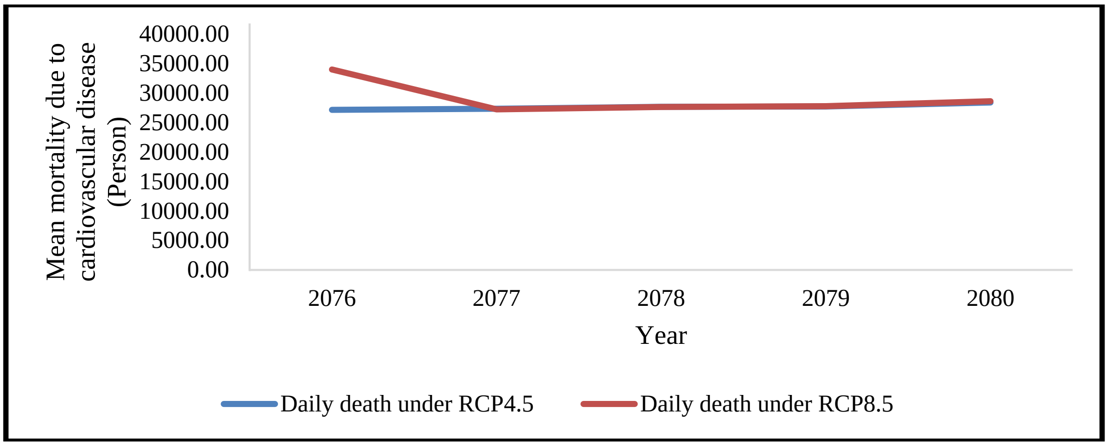

Figure 5: The line graph of attributable daily death (ADD) due to cardiovascular disease under RCP4.5 and RCP8.5

Figure 6 shows the box plots of ADD under RCP4.5 and RCP8.5 in 2076, 2077, 2078, 2079 and 2080. Many outliers in 2076, 2077, 2078, 2079 and 2080 can be detected. The projected number of ADD for RCP4.5 and RCP4.5 typically similar and vary widely as there are many outliers on the left whisker. RCP8.5 showed higher projected number of ADD on average for all years compared to RCP4.5. Generally, the shape of the distribution between the years 2076 and 2080 are negatively skewed. The projected number of ADD for both RCPs could reach up to more than 40,000 people. However, more than 75% projects lower number of ADD with less than 10,000 people died.

7. Conclusion

In summary, quantile mapping technique has shown the ability to capture the variability in GCM as well as quantifying the biases. The projected trend of heat-related deaths under RCP4.5 is lower than the deaths under RCP8.5. This might be due to the attributable change in mortality of CVD for a specified change in temperature which only involves the calculation of exposure-response relationship. Specifically, the lag-response relationship was not considered in the calculation different delay effect of heat could not be captured. Natural cubic B-spline of day of the year with equally spaced knots with six degree of freedom (df) is able to control seasonality while the natural cubic B-spline of time with eight degree of freedom (df) is able to control long-term trends. For future works, the location parameter, θ will be considered in Gamma distribution to describe the central values such as mean, median and mode. Besides, lag-response relationship could also be considered in the calculation of the attributable change in mortality due to cardiovascular diseases for a specified change at each temperature.

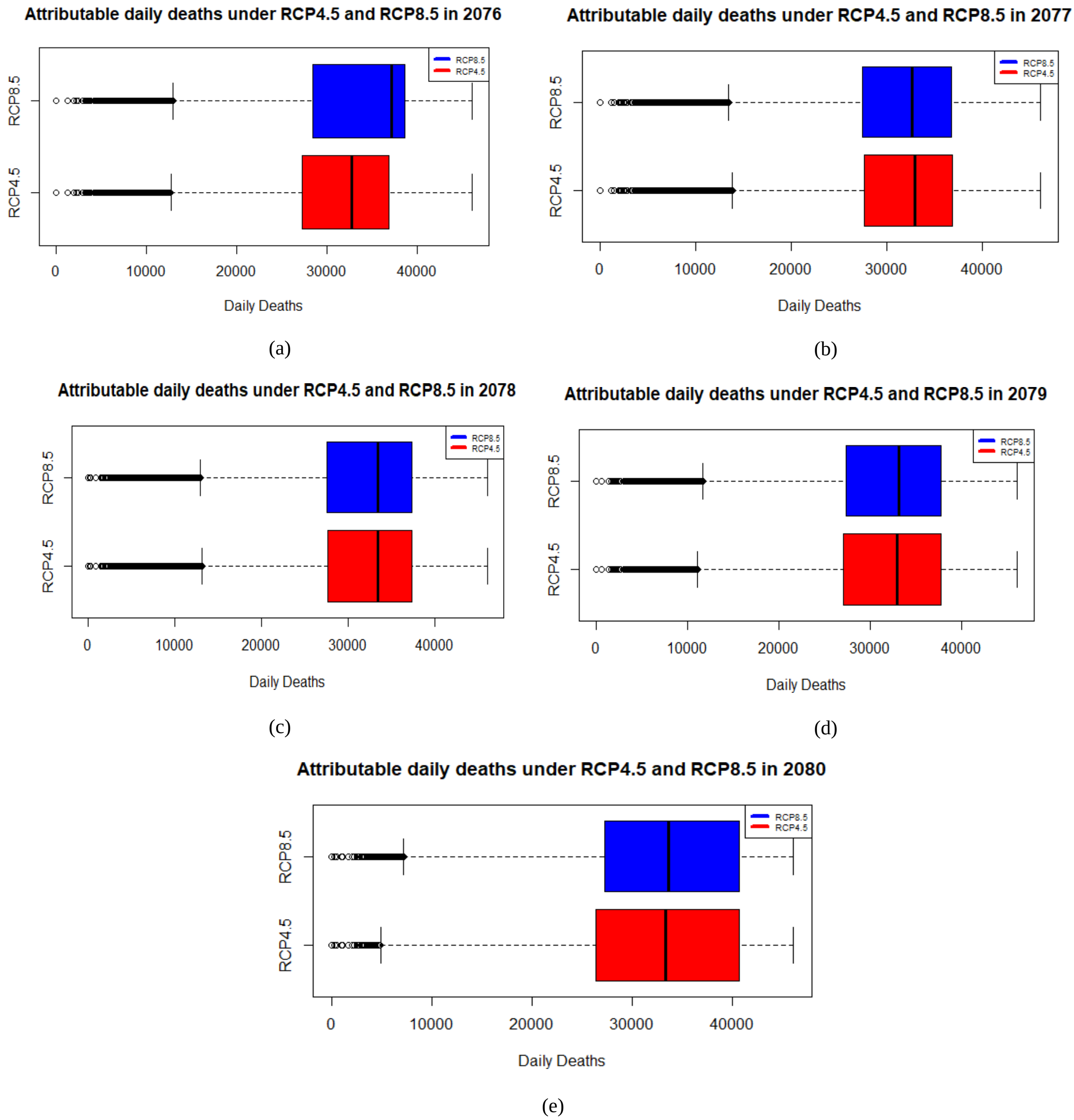

Figure 6: The box plots of attributable daily death (ADD) under RCP4.5 and RCP8.5 in (a) 2076, (b) 2077, (c) 2078, (d) 2079 and (e) 2080

Acknowledgments

The observed gridded data were sourced from Wong *et al.* (2011). This study was fully supported by the Ministry of Education (MOE) through Fundamental Research Grant (FRGS/1/2018/STG06/UPM/02/5), Vote No: 5540130. Thank you to Assoc. Prof. Dr. Liong CY and the editors of Journal of Quality Measurement and Analysis for their useful and helpful suggestions and comments.

References

Abatzoglou J.T. & Brown T.J. 2012. A comparison of statistical downscaling methods suited for wildfire applications. *International Journal of Climatology* **32**: 772-780.

Abdullah W.M.S.W., Yusoff Y.S., Basir N. & Yusuf M.M. 2017. Mortality rates due to coronary heart disease by specific sex and age groups among Malaysians. *Proceeding of the World Congress on Engineering and Computer Science*, pp. 736-741.

Ajaaj A.A., Mishra A.K. & Khan A.A. 2016. Comparison of bias correction techniques for GPCC rainfall data in semi-arid climate. *Stochastic Environmental Research and Risk Assessment* **30**(6): 1659-1675.

Chen K., Horton R.M., Bader D.A., Lesk C., Jiang L., Jones B., Zhou L., Chen X., Bi J. & Kinney P.L. 2017. Impact of climate change on heat-related mortality in Jiangsu Province, China. *Environmental Pollution* **224**: 317-325.

Crimmins A., Balbus J., Gamble J.L., Beard C.B., Bell J.E., Dogden D., Eisen R.J., Fann N., Hawkins M.D., Herring S.C., Jantarasami L., Mills D. M., Saha S., Sarofim M.C., Trtanj J. & Ziska L. (eds.). 2016. *The Impacts of Climate Change on Human Health in the United State: A Scientific Assessment.* Washington DC: U.S. Global Change Research Program.

Department of Statistics Malaysia. 2016. Population projection (revised), Malaysia, 2010-2040.

Gasparrini A., Armstrong B. & Kenward M.G. 2010. Distributed lag non-linear model. *Statistics in Medicine* **29**(12): 2224-2234. doi: 10.1002/sim.3940.

Husak G.J., Michaelsen J. & Funk C. 2007. Use of the gamma distribution to represent monthly rainfall in Africa for drought monitoring applications. *International Journal of Climatology* **27**(7): 935-944.

Kei H.M. 2017. Statistics Causes of Deaths, Malaysia, 2017. Department of Statistics Malaysia, 31 Oktober.

Luber G. & McGeehin M. 2008. Climate change and extreme heat events. *American Journal of Preventive Medicine* **35**(5): 429-435.

Tang K.H.D. 2019. Climate change in Malaysia: Trends, contributors, impacts, mitigation and adaptations. *Science of The Total Environment* **650**: 1858-1871.

Teutschbein C. & Seibert J. 2012. Bias correction of regional climate model simulations for hydrological climate change impact studies: Review and evaluation of different methods. *Journal of Hydrology* **456-457**: 12-29.

Wayne G.P. 2013. The Beginner's Guide to Representative Concentration Pathways. Skeptical Science. http://www.skepticalscience.com/docs/RCP Guide.pdf (12 December 2019).

Wong C.L., Venneker R., Jamil A.B. & Uhlenbrook S. 2011. Development of a gridded daily hydrometeorological data set for Peninsular Malaysia. *Hydrological Processes* **25**(7): 1009-1020.

World Health Organization. 2018. Noncommunicable diseases country profiles 2018.

Department of Mathematics
Faculty of Science
Universiti Putra Malaysia
43400 UPM Serdang
Selangor DE, MALAYSIA
*E-mail: ainaizzati05@gmail.com, syafrina@upm.edu.my**

UTM Razak School of Engineering and Advanced Technology
Universiti Teknologi Malaysia
54100 Kuala Lumpur, MALAYSIA
E-mail: zaida.kl@utm.my

Faculty of Science and Marine Environment
Universiti Malaysia Terengganu
21030 Kuala Nerus
Terengganu DI, MALAYSIA
Email: jingxiang@umt.edu.my

Institut Penyelidikan Air Kebangsaan Malaysia (NAHRIM)
Kementerian Alam Sekitar dan Air (KASA)
Lot 5377 Jalan Putra Permai
43300 Seri Kembangan
Selangor DE, MALAYSIA
Email: syazwan@nahrim.gov.my

Received: 9 March 2020
Accepted: 29 October 2020

[*]Corresponding author